

Fracability Evaluation Method of a Fractured-Vuggy Carbonate Reservoir in the Shunbei Block

Yan Zhang, Lufeng Zhang, Jiayuan He, Hao Zhang,* Ximin Zhang, and Xiang Liu



Cite This: *ACS Omega* 2023, 8, 15810–15818

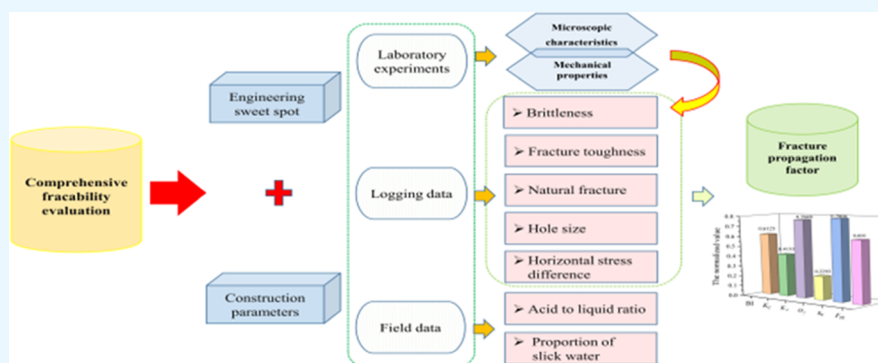


Read Online

ACCESS |

Metrics & More

Article Recommendations



ABSTRACT: The fracability of carbonate reservoirs is a key indicator for evaluating whether reservoirs can be effectively fractured. Taking the fractured-vuggy carbonate reservoir in the Shunbei block as an example, the microscopic characteristics and mechanical properties of this reservoir were analyzed. The test results showed that the core microstructure is relatively dense, the micropores and microfractures are developed, and the mineral composition is characterized by “high carbonate and few impurities”. The compressive strength, Young’s modulus, and Poisson’s ratio of the rock increased with the increase in the confining pressure. Poisson’s ratio is more sensitive to confining pressure than Young’s modulus and shows the ductile transformation tendency from a low confining pressure to a high confining pressure. Considering the difficulty of forming a complex fracture network, we put forward a “fracture propagation factor” equation constructed with five main factors, including brittleness, fracture toughness, natural fracture, hole size, and horizontal stress difference, and then the fracture propagation factor of Yijianfang formation is calculated to be greater than 0.5. It is known that the Yijianfang formation has higher fracability. On this basis, combined with the construction parameters, a model for evaluating the fracability of a fractured-vuggy carbonate reservoir was established. The comprehensive fracability of four wells in the Shunbei block was calculated by the model. From the calculation results, the comprehensive fracability index of SHB43X was 0.5406 and greater than that of the other three wells, which has a high correlation with the production after fracturing.

1. INTRODUCTION

Carbonate reservoirs are rich in oil and gas resources and have great potential for exploration and development.¹ Carbonate reservoirs mainly include three types: pore type, fracture-pore type, and fractured-vuggy type. Among them, fractured-vuggy carbonate reservoirs are the focus of oil and gas development.² In this type of reservoir, due to the existence of natural fractures, pore bodies, and fracture-cavity systems, serious fluid leakage will occur, resulting in wellbore instability and reservoir damage. Therefore, some scholars have studied the performance of fluids entering the wellbore, such as drilling fluid, completion fluid, and fracturing fluid. Murtaza et al. found that okra powder can control fluid loss in water-based drilling fluids and okra mucilage can prevent shale swelling.^{3,4} Tariq et al. took dicationic surfactants as an additive in fracturing fluids to mitigate clay swelling and used polyoxyethylene quaternary ammonium gemini surfactants as

a completion fluid additive to mitigate formation damage.^{5–7} The related experiments of the chelating agent as an acid fracturing fluid were carried out, and it was concluded that the chelating agent can etch the created fracture length more than HCl acid.⁸ Further research pointed out that the chelating agent is suitable for calcite rocks and not suitable for less reactive rocks such as dolomites.⁹

In addition, the presence of fractures and vugs will change the nearby stress field, which makes it difficult to predict its

Received: March 24, 2023

Accepted: April 12, 2023

Published: April 20, 2023



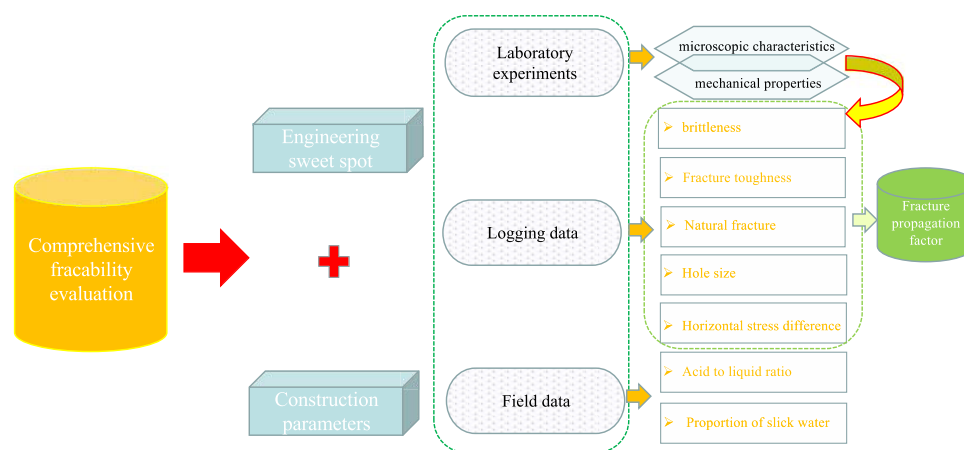


Figure 1. Workflow diagram of comprehensive fracability evaluation.

fracture pressure. Tariq et al. predicted the fracture pressure by machine learning method, and the prediction results are highly accurate.¹⁰ At the same time, the change in the stress field will affect the expansion mode and extension path of hydraulic fracture. The hydraulic fracture generated by conventional fracturing does not necessarily expand along the envisaged path and communicate with the hole, resulting in poor fracturing effect and increased fracturing resource cost. Therefore, it is urgent to determine the influencing factors of fracability and establish a scientific fracability evaluation model for a fractured-vuggy carbonate reservoir.

At present, the evaluation methods of the fracture-vuggy carbonate reservoir fracturing effect are mainly divided into the following categories. First, the influence of various factors on the fracturing effect of the target layer is analyzed and calculated by the mathematical method. For example, Hui et al. sorted the factors affecting the acid fracturing of carbonate reservoirs in Tarim by a gray correlation method. It is considered that the fracture density, reservoir level, natural γ , and lateral resistivity ratio have a significant influence on the results.¹¹ Yan et al. established a comprehensive fracability index based on rock brittleness, compressive strength, and fracture toughness for tight carbonate reservoirs.¹² Second, the influence of various factors on the fracture propagation of carbonate rocks is simulated by laboratory experiments. For example, Xinyong,¹³ on the basis of a hydraulic fracturing physical simulation experiment, according to the characteristics of fracture-cavity carbonate, put forward the evaluation index of fracturing effect, namely, fracture-cavity communication coefficient, and studied the influence of horizontal stress difference on the fracturing effect. Bing et al.¹⁴ carried out hydraulic fracturing tests using natural cores and artificial cores to monitor the physical process of fracture propagation and pointed out the influencing factors of hydraulic fracture propagation. Finally, microseismic technology, logging data, or construction parameters were used to determine the effect of a fracturing target layer. For example, Fisher et al.^{15,16} used microseismic fracture monitoring technology to analyze the complex network expansion of hydraulic fractures in the plane and depth. They believe that the larger the volume of fracturing fluid, the larger the spread area of microseismic events and the higher the production. Mayerhofer et al.^{17,18} studied the hydraulic fracture morphology of Barnett shale in combination with microseismic technology, established the SRV calculation method, and proposed the concept of

“stimulated reservoir volume”. It is considered that the larger the stimulated reservoir volume, the better the stimulation effect. The concept realizes the quantitative evaluation of the fracturing effect.

The above evaluation methods of the fracturing effect ignore the influence of fracture-cavity development degree and fracturing characteristic parameters (such as the acid-to-liquid ratio and the proportion of slippery water) on the fracturing effect of fracture-vuggy carbonate reservoirs, so it is difficult to evaluate the fracturing effect of such reservoirs scientifically and systematically.

Zehua et al.¹⁹ pointed out that the fracability of carbonate reservoirs needs to consider the reservoir reconstruction volume and the difficulty of forming a complex fracture network. Therefore, this paper takes the fractured-vuggy carbonate reservoir in the Shunbei block as the research object, considering the influence of brittleness, fracture toughness, natural fracture, hole size, and horizontal stress difference on the fracture extension of fractured-vuggy carbonate reservoir, the concept of “fracture propagation factor” is proposed. On this basis, combined with its mechanical characteristics and fracturing parameters, a model for evaluating the fracability and fracability grading standard suitable for fractured-vuggy carbonate reservoirs is established. The workflow is illustrated in Figure 1.

2. MICROSCOPIC CHARACTERISTICS AND MECHANICAL PROPERTIES

In the first part of the study, laboratory experiments were conducted to study the microscopic characteristics and mechanical properties of the fractured-vuggy carbonate rocks.

2.1. Mineral Composition. The rock sample is from the Ordovician Yijianfang Formation in the Shunbei block. The lithology is mainly yellow-gray micrite limestone, gray micrite limestone, gray sandy lithic micrite limestone, and gray sandy micritic limestone (Figure 2). According to the X-ray diffraction (XRD) test results of the rock samples, the content of calcite is 99.2%, the content of quartz is 0.4%, and the content of dolomite is 0.3%. The content of brittle minerals is extremely high, and the mineral composition is characterized by “high carbonate and few impurities”. It implies that the Yijianfang Formation has strong fracability.

2.2. Microstructure. The study of the microscopic characteristics of rocks can deepen the understanding of the laws of macroscopic characteristics, which is of great



Figure 2. Lithology of Ordovician Yijianfang Formation in the Shunbei block. Photograph courtesy of 'Hao Z. and Yan Z'. Copyright 2022.

significance to engineering construction and engineering application. Therefore, the change rules of the rock's microscopic characteristics before and after acidification (immersed in HCL acid until saturation) were studied. The scanning electron microscopy (SEM) results of the microstructure of the rock samples are shown in Figure 3. It can be found that the core microstructure is relatively dense before acidification, and the micropores and microfractures are developed. After acidification, the micropores and microfractures of the core increase, and some pores are connected. In addition, the acid solution etches the fractures differently, forming a heterogeneous acid-etched fracture surface. It is inferred that the Yijianfang Formation has good fracability and acid fracturing has a good effect on increasing production.

2.3. Compressive Strength Test. The uniaxial and triaxial compressive strength tests of the rock samples (taken from the Yijianfang Formation of SHB41X) were carried out under different confining pressures (0, 30, 60 MPa). The stress–strain curve of the specimen is shown in Figure 4. The stress–strain curves of each group of rock samples have the same trend, and it shows the characteristics of “short compaction section-long linear elastic section”. Then, entering the yield stage, the stress drops sharply after reaching the peak until failure, and the failure stage shows strong brittleness characteristics.

With the increase in the confining pressure, the peak point of stress–strain moves to the upper right, the peak stress and strain increase, the slope after the peak slows down, and shows a ductile transformation tendency from a low confining

pressure to a high confining pressure. At the same time, Young's modulus and Poisson's ratio increase with the increase of confining pressure, and Poisson's ratio is more sensitive to confining pressure than Young's modulus. The change of elastic parameters under different confining pressures is shown in Figure 5.

The dynamic Young's modulus and Poisson's ratio of the sample were calculated by acoustic logging data (Figure 6) and fitted with the static Young's modulus and Poisson's ratio of the laboratory test (Figure 7). The results show that the dynamic elastic parameters are greater than the static elastic parameters, the dynamic and static Young's moduli are quite different, and the dynamic and static Poisson's ratios are approximately equal. The inherent cause of this difference is the rock composition and structure, such as fissure, soft pore, and weak contact between rock grains, and the existence of pore fluid in rock.

2.4. Tensile Strength Test. Due to the limited core, the test data of five strips in Shunbei are adopted, and the experimental data are shown in Table 1. The experimental data show that there is a big difference in the tensile strength of the Yijianfang Formation of the five strips, which is between 2.45 and 6.63 MPa, which may be related to its strong heterogeneity. In order to reduce the error, its mean value of 4.22 MPa is adopted. At the same time, the tensile strength of different buried depths was calculated by using acoustic logging data (data from SHB41X), as shown in Figure 8. The average tensile strength of Yijianfang Formation is 5.38 MPa.

3. FRACABILITY EVALUATION

The factors affecting the fracture propagation of a fractured-vuggy carbonate reservoir were analyzed, and it was concluded that the hole size has a key influence on the fracture extension. This paper presents an application of logging data to quantitatively characterize the hole size, and we establish a model for calculating the fracture propagation factor by analytic hierarchy process (AHP), which can directly reflect the fracability of reservoirs to a certain extent.

3.1. Factors Influencing Fracture Propagation. The fracture-vuggy carbonate reservoirs are quite different from the hydraulic fracture propagation path and fracture morphology of homogeneous reservoirs. The hydraulic fracture propagation path and fracture morphology of this type of reservoir are more complex and diverse. Related

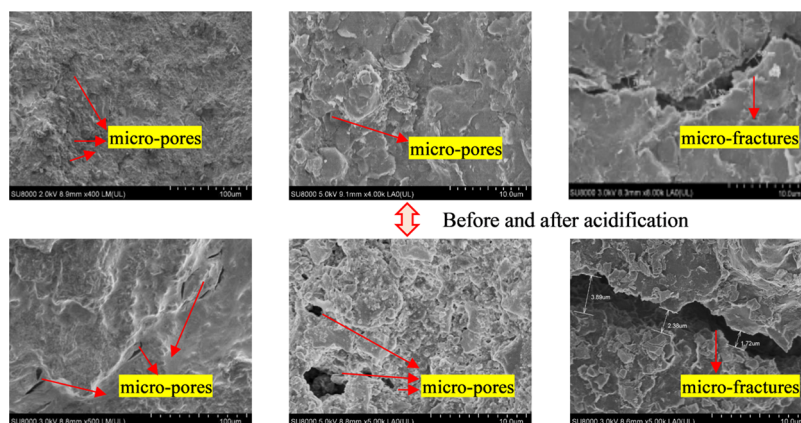


Figure 3. Microstructure of samples from the Yijianfang Formation before and after acidification.

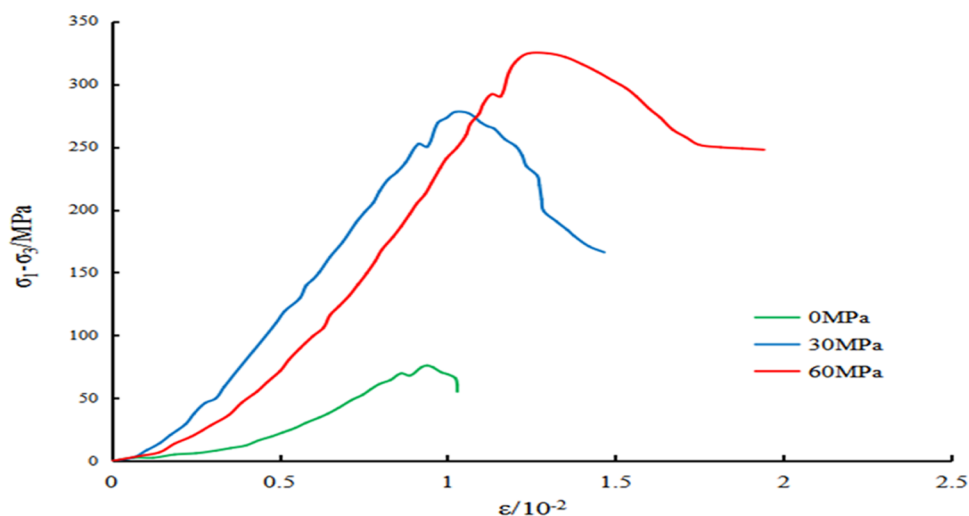


Figure 4. Stress–strain curves of the specimen.

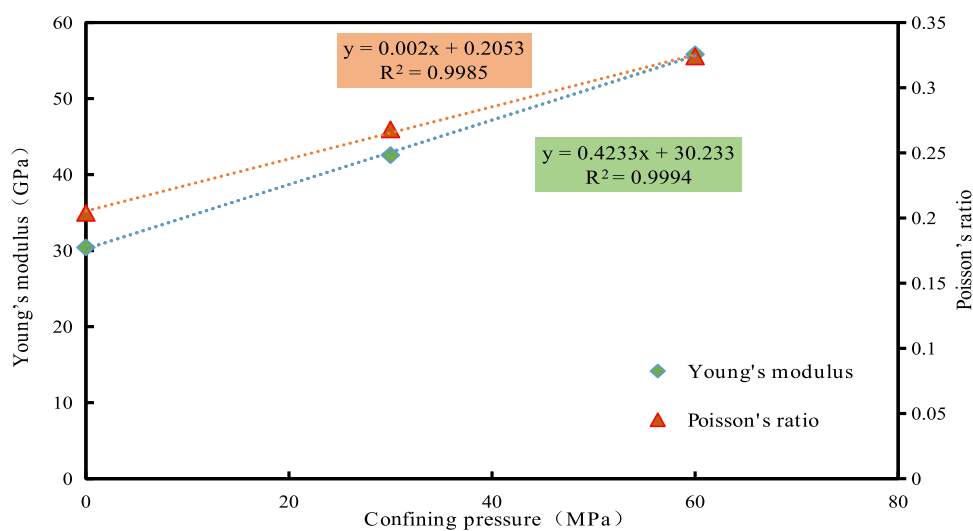


Figure 5. Changes of elastic parameters under different confining pressures.

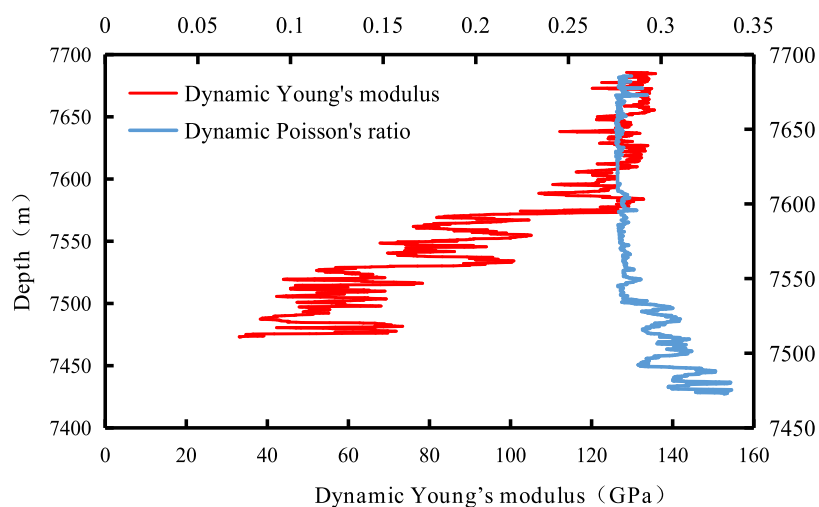


Figure 6. Dynamic Young's modulus and dynamic Poisson's ratio.

studies^{20–23} have shown that brittleness, fracture toughness, natural fracture, hole size, and horizontal stress difference have significant effects on fracture propagation.

3.1.1. Brittleness. The brittleness of rock is an important reference index for fracturing. The greater the brittleness of the rock, the more microfractures are induced near the main

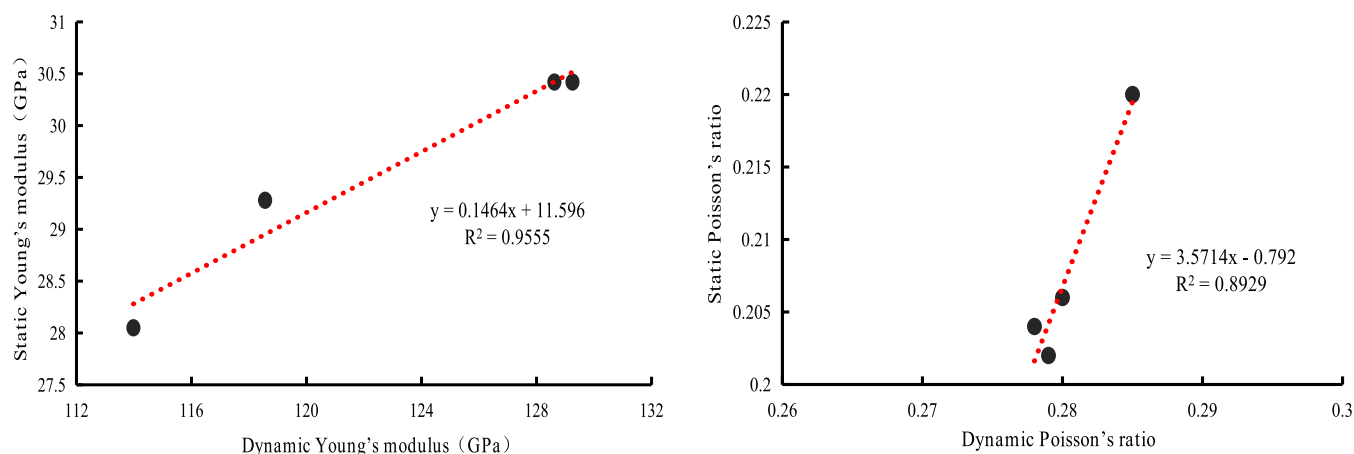


Figure 7. Fit of dynamic and static Young's modulus and Poisson's ratio.

Table 1. Tensile Strength Test of Five Strips in Shunbei

sample	results		
	F (N)	tensile strength (MPa)	the average tensile strength (MPa)
s501-1-19-74 (7653.41–7653.54 m)	2225.00	4.42	4.22
s501-1-23-74 (7653.73–7653.81 m)	1557.50	3.38	
s501-1-25-74 (7653.86–7653.94 m)	1335.00	2.45	
s501-1-62-74 (7656.38–7656.46 m)	2447.50	6.63	

cracks generated by hydraulic fracturing, and it is easier to form a complex fracture network. The calculation methods of rock brittleness are mainly based on mineral composition and elastic parameters. The mineral composition method is based on the content of brittle minerals in rocks, as shown in eq 1. Brittle minerals mainly include calcite, quartz, and feldspar.²⁴ The elastic parameter method is based on Young's modulus and Poisson's ratio. High Young's modulus and low Poisson's ratio often mean strong brittleness. According to the Rickman brittleness index evaluation method,²⁵ Young's modulus and Poisson's ratio are normalized, and the brittleness is described by the mean of the two, as shown in eq 4.^{24,25}

$$B_W = \frac{w_{qtz} + w_{feld} + w_{cal}}{w_{tot}} \quad (1)$$

$$E_n = \frac{E - E_{min}}{E_{max} - E_{min}} \quad (2)$$

$$\mu_n = \frac{\mu_{max} - \mu}{\mu_{max} - \mu_{min}} \quad (3)$$

$$B_E = \frac{E_n + \mu_n}{2} \quad (4)$$

In order to reduce the error caused by the limitations of the two methods, this paper calculates the rock brittleness by eq 5.

$$BI = \frac{B_W + B_E}{2} \quad (5)$$

where BI, B_W , and B_E are the comprehensive brittleness index, brittleness index based on mineral composition, and brittleness index based on elastic parameters, respectively; w_{qtz} , w_{feld} , w_{cal} , and w_{tot} represent the composition quality of quartz, feldspar, calcite, and total mineral, respectively; and E_n and μ_n are the normalized Young's modulus and Poisson's ratio, respectively.

3.1.2. Fracture Toughness. Fracture toughness can characterize the ability of fracture extension after fracture initiation. The smaller the fracture toughness value, the less energy is required for the extension of hydraulic fractures, the easier it is to form a complex fracture network and the

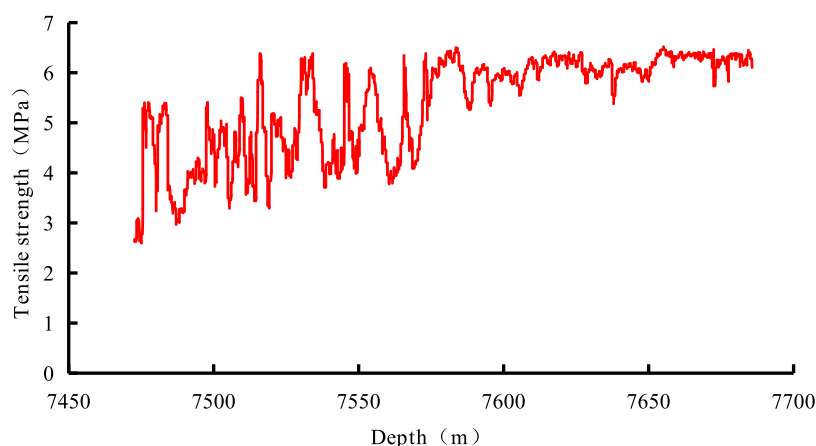


Figure 8. Variation of tensile strength with buried depth.

stronger the fracability. During the hydraulic fracturing process, the formed fractures are mostly Mode I and Mode II. Based on a large number of experiments, Yan et al.²⁶ established the relationship between Mode I and Mode II fracture toughness and reservoir confining pressure and tensile strength, as follows.²⁶

$$\begin{aligned} K_{IC} &= 0.2176P_C + 0.0059S_t^3 + 0.0923S_t^2 + 0.517S_t \\ &\quad - 0.3322 \\ K_{IIC} &= 0.0956P_C + 0.1383S_t - 0.082 \end{aligned} \quad (6)$$

In this paper, the fracture toughness is characterized by the standardized mean value of Mode I and Mode II fracture toughness. That is

$$K_C = \frac{K_{IC-n} + KI_{IIC-n}}{2} \quad (7)$$

K_C is the fracture toughness index; K_{IC} and K_{IIC} are Mode I and Mode II fracture toughness values, respectively; K_{IC-n} and KI_{IIC-n} are the normalized fracture toughness values, respectively; P_C is the reservoir confining pressure; and S_t is the tensile strength.

3.1.3. Natural Fracture. Natural fractures will provide favorable conditions for the expansion of hydraulic fractures. The pressure required for hydraulic fracture propagation in the presence of natural fractures is significantly less than the fracture pressure required to open new fractures, and the distribution of natural fractures will significantly affect the cross-communication of primary and secondary fractures and the scale of fracture networks formed.

At present, the identification and quantitative evaluation of natural fractures are mostly based on logging data, while the single conventional logging method and the triple porosity logging have a poor response in carbonate reservoirs with developed dissolution pores, local fractures, and complex pore structures.²⁷ Therefore, a variety of conventional logging curve reconstruction methods are used. Xiaoling Xiao established a reconstruction feature (DACR) based on the variation of conventional logging curves with fracture development, which can effectively identify fracture development characteristics.²⁸ The natural fracture index G_f is characterized by the value of reconstructed characteristic (DACR).²⁸

$$DACR = \frac{AC \cdot CNL}{DEN \cdot RD \cdot RS} \quad (8)$$

where DACR denotes the reconstruction of features and AC, CNL, DEN, RD, and RS are the normalized acoustic time difference, the normalized compensated neutron, the normalized bulk density, the normalized deep, and the normalized shallow lateral resistivity, respectively.

3.1.4. Hole Size. The larger the size of the hole, the more concentrated the stress around it and the more difficult it is for the fracture to break through the expansion of the vugs. In this paper, the hole size of the fractured-vuggy carbonate reservoir is characterized by using a variety of logging response pore identification indexes²⁹ including comprehensive resistivity invasion correction ratio, curve change rate, and secondary porosity method²⁹

$$\begin{aligned} R_{SD} &= \frac{R_t - RS}{RS} \\ R_t &= 2.589RD - 1.589RS \\ AC_{VAR} &= \frac{(|AC_{i+1} - AC_i| + |AC_{i-1} - AC_i|)}{2} \\ DS &= \text{LOG}(RD) - \text{LOG}(RS) \end{aligned} \quad (9)$$

$$R_H = \frac{R_{SD} + AC_{VAR} + DS}{3} \quad (10)$$

where R_{SD} is the true resistivity ratio of the strata after intrusion correction; RD and RS are deep and shallow lateral resistivity, respectively; R_t is the true resistivity of the strata after intrusion correction; AC_{VAR} is the change rate of the acoustic time difference; AC_i is the response value of the acoustic time difference curve at the current depth point; AC_{i+1} and AC_{i-1} are the response values of the acoustic time difference curve at the two depth point respectively; and DS is the secondary porosity.

3.1.5. Horizontal Stress Difference. The high or low ground stress affects the shape of the fracturing fracture. The hydraulic fracture changes longitudinally under the influence of the minimum horizontal principal stress and expands along the direction of the maximum horizontal principal stress. Generally speaking, the smaller the horizontal stress difference, the easier it is to form a complex fracture network. In deep strata, the difficulty of forming a complex fracture network is characterized by the horizontal stress difference coefficient.

$$K_\sigma = \frac{\sigma_1 - \sigma_3}{\sigma_3} \quad (11)$$

where K_σ is the horizontal stress difference coefficient and σ_1 and σ_3 are the maximum horizontal principal stress and the minimum horizontal principal stress, respectively (MPa).

3.2. Fracture Propagation Factor. According to the related studies,^{30–32} the relative importance of various influencing factors (brittleness, fracture toughness, natural fracture, hole size, and horizontal stress difference) to fracture extension was determined and assigned. The weight coefficient of each influencing factor is determined by the judgment matrix (Table 2) constructed by the analytical hierarchy process, and the fracture propagation factor equation is established.

The sum-product method is used to calculate the weight. The calculation results are shown in Table 3, and the consistency index (CR) is used to test the consistency of the

Table 2. Judgment Matrix of Fracture Propagation Evaluation

factor	brittleness	fracture toughness	horizontal stress difference	natural fracture	hole size
brittleness	1	1/3	1/4	1/5	1/7
fracture toughness	3	1	1/4	1/5	1/6
horizontal stress difference	4	4	1	1/2	1/5
natural fracture	5	5	2	1	1/3
hole size	7	6	5	3	1

Table 3. Corresponding Weights of Each Factor

	BI	K_C	K_σ	G_f	R_H	CR
weights	0.037	0.087	0.189	0.259	0.428	0.070

judgment matrix. The consistency index (CR) is less than 0.1, and the constructed judgment matrix is considered to be reasonable.³³ According to the analysis results, CR was $0.07 < 0.1$, passing the consistency test. The weights of brittleness, fracture toughness, horizontal stress difference coefficient, natural fracture, and hole size are 0.037, 0.087, 0.189, 0.259, and 0.428, respectively.

$$CR = \frac{CI}{RI} \quad (12)$$

$$CI = (\lambda_{\max} - n)/(n - 1) \quad (13)$$

$$\lambda_{\max} = \sum_{i=1}^n \frac{|Aw_i|}{nw_i} \quad (14)$$

4. RESULTS AND DISCUSSION

The fracture propagation factor is calculated by eq 15. Then, the influencing factors are substituted into the model after range transformation, and the calculation results are shown in

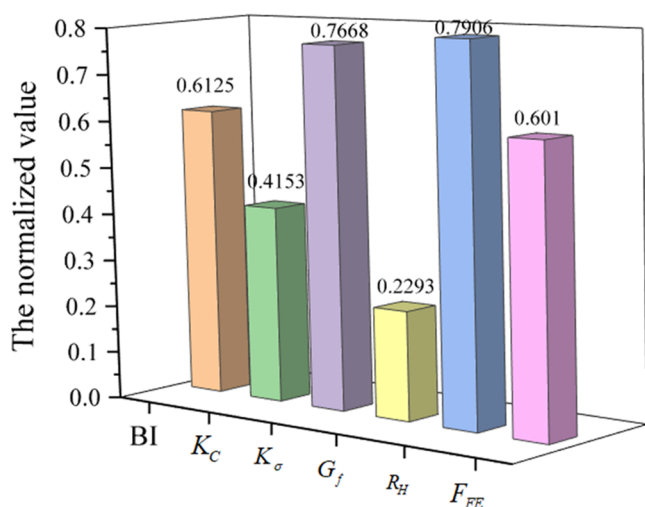


Figure 9. Fracture propagation factor of Ordovician Yijianfang formation.

Figure 9. Large fracture propagation factor reveals engineering sweet spot.

$$F_{FE} = 0.037BI + 0.087K_C + 0.189K_\sigma + 0.259G_f + 0.428R_H \quad (15)$$

where F_{FE} is the fracture propagation factor, BI is the brittleness, K_C is the fracture toughness, K_σ is the horizontal stress difference coefficient, G_f is the natural fracture index, and R_H is the hole size.

In view of the fact that the fracture propagation factor has been limited to near-wellbore zone, a comprehensive model of fracability was established by taking into account both geology and construction parameters. The construction parameters mainly consider the characteristic parameter

acid–liquid ratio and the proportion of slippery water. The comprehensive fracability index is calculated by eq 16.

$$FI = \alpha F_{FE} + \beta V_{acid} + \gamma \gamma_{sw} \quad (16)$$

where FI is the comprehensive fracability index, V_{acid} is the acid-to-liquid ratio, γ_{sw} is the proportion of slick water, and α , β , and γ are the corresponding weights, where $\alpha = 0.7$, $\beta = 0.15$, and $\gamma = 0.15$.

Based on the above comprehensive fracability evaluation model of the fractured-vuggy carbonate reservoir, combined with the field data, we calculate the comprehensive fracability index of four wells in the target block. The results are shown in Table 4.

Table 4. Comprehensive Fracability Evaluation of the Fractured-Vuggy Carbonate Reservoir

wells	fracture propagation factor (F_{FE})	acid–liquid ratio (V_{acid})	proportion of slippery water (γ_{sw})	comprehensive fracability (FI)
SHB41X	0.601	0.64	0.14	0.5377
SHB43X	0.558	0.78	0.22	0.5406
SHB1-H	0.556	0.65	0.15	0.5092
SHB2-H	0.579	0.43	0.28	0.5118

Comparing the production after acid fracturing and the comprehensive fracability index, it is found that they have a good correlation (Figure 10). SHB43X has the highest comprehensive fracability index, with the daily gas production of 409,000 cubic meters and the daily oil production of 317.2 tons. The SHB1-H comprehensive fracability index is lower than those of other wells, with a daily gas production of 186,000 cubic meters and a daily oil production of 87.6 tons. Field application showed that the comprehensive fracability evaluation method is reliable and practicable.

On the basis of the grading standard of fracability by Hongwei et al.,³⁴ a comprehensive fracability evaluation standard of acid fracturing for fractured-vuggy carbonate rocks is established. It is considered that when the comprehensive fracability index is lower than 0.3, the fracability of the fractured-vuggy carbonate reservoir is poor. If the comprehensive fracability index is between 0.3 and 0.5, the fracability is acceptable, and if the comprehensive fracability index is higher than 0.5, the fracability is good.

5. CONCLUSIONS

- (1) The mineral composition is characterized by high carbonate and few impurities. The microstructure is relatively dense, and the micropores and microfractures are developed. After acidification, micropores and microfractures increase. The compressive strength, Young's modulus, and Poisson's ratio of the rock increase with the increase in the confining pressure.
- (2) It is considered that hole size is the main controlling factor of fracture propagation in fractured-vuggy carbonate reservoirs. The fracture propagation factor can quantitatively characterize the difficulty of fracture propagation in fractured-vuggy carbonate rocks and directly reflect the fracability of reservoirs to a certain extent.
- (3) The comprehensive evaluation model for evaluating the fracability of fractured-vuggy carbonate reservoir is

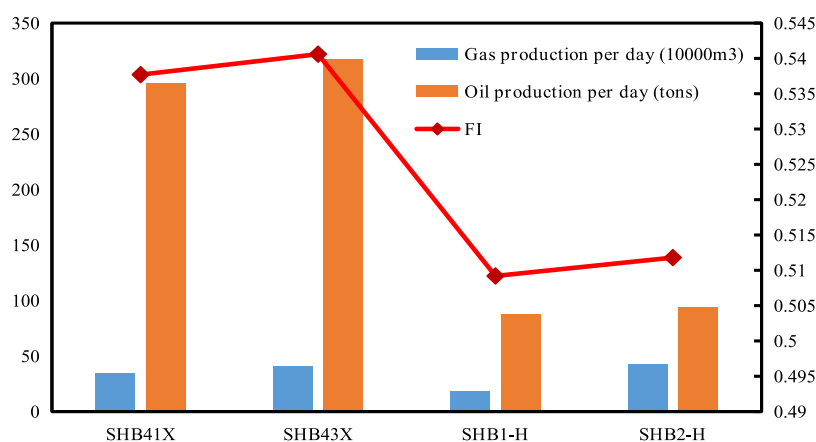


Figure 10. Relationship between FI and the production after acid fracturing.

constructed and the standard of fracability for acid fracturing is established. It is considered that the comprehensive fracability index of the Ordovician reservoir in the Shunbei block is greater than 0.5, which is suitable for acid fracturing.

AUTHOR INFORMATION

Corresponding Author

Hao Zhang – College of Petroleum Engineering of Yangtze University, Wuhan 430100 Hubei, China; orcid.org/0000-0003-1985-8966; Email: 1902023423@qq.com

Authors

Yan Zhang – Key Laboratory of Marine Oil & Gas Reservoirs Production, Petroleum Exploration and Production Research Institute, Sinopec, Beijing 102206, China; College of Petroleum Engineering of Yangtze University, Wuhan 430100 Hubei, China

Lufeng Zhang – Key Laboratory of Marine Oil & Gas Reservoirs Production, Petroleum Exploration and Production Research Institute, Sinopec, Beijing 102206, China; orcid.org/0000-0003-0630-8519

Jiayuan He – Key Laboratory of Marine Oil & Gas Reservoirs Production, Petroleum Exploration and Production Research Institute, Sinopec, Beijing 102206, China

Ximin Zhang – Drilling Technology Research Institute, Sinopec Shengli Oilfield Service Corporation, Deyang 618000 Sichuan, China

Xiang Liu – Petroleum Engineering Technology Research Institute, Sinopec JiangHan Oilfield Corporation, Wuhan 433124 Hubei, China

Complete contact information is available at: <https://pubs.acs.org/10.1021/acsomega.3c02000>

Notes

The authors declare no competing financial interest.

ACKNOWLEDGMENTS

Y.Z., H.Z., L.Z., and J.H. thank the Key Laboratory of Marine Oil & Gas Reservoirs Production, Sinopec, for the Research Funding through grant 33550000-22-FW2099-0004.

NOMENCLATURE

BI the comprehensive brittleness index, dimensionless

B_W	the brittleness index based on mineral composition, dimensionless
B_E	the brittleness index based on elastic parameters, dimensionless
w_{qtz}	the composition quality of quartz, dimensionless
w_{feld}	the composition quality of feldspar, dimensionless
w_{cal}	the composition quality of calcite, dimensionless
w_{tot}	the composition quality of total mineral, dimensionless
E_n	the normalized Young's modulus, dimensionless
μ_n	the normalized Poisson's ratio, dimensionless
K_C	the fracture toughness index, dimensionless
K_{IC}	the Mode I fracture toughness values, $MPa \cdot m^{1/2}$
K_{IIc}	the Mode II fracture toughness values, $MPa \cdot m^{1/2}$
K_{IC-n}	the normalized Mode I fracture toughness values, dimensionless
K_{IIc-n}	the normalized Mode II fracture toughness values, dimensionless
P_C	the reservoir confining pressure, MPa
S_t	the tensile strength, MPa
DACR	the reconstruction of features, dimensionless
AC_n	the normalized acoustic time difference, dimensionless
CNL_n	the normalized compensated neutron, dimensionless
DEN_n	the normalized bulk density, dimensionless
RD_n	the normalized deep lateral resistivity, dimensionless
RS_n	the normalized shallow lateral resistivity, dimensionless
R_{SD}	the true resistivity ratio of the strata after intrusion correction, dimensionless
RD	the deep lateral resistivity, $\Omega \cdot m$
RS	the shallow deep lateral resistivity, $\Omega \cdot m$
R_t	the true resistivity of the strata after intrusion correction, $\Omega \cdot m$
AC_{VAR}	the change rate of acoustic time difference, dimensionless
DC	the secondary porosity, $\Omega \cdot m$
K_σ	the horizontal stress difference coefficient, dimensionless
σ_1	the maximum horizontal principal stress, MPa
σ_3	the minimum horizontal principal stress, MPa
R_H	the size of the hole, dimensionless
G_f	the natural fracture index, dimensionless
CR	the consistency index, dimensionless
F_{FE}	the fracture propagation factor, dimensionless

FI	the comprehensive compressibility index, dimensionless
V_{acid}	the acid to liquid ratio, dimensionless
γ_{sw}	the proportion of slick water, dimensionless

REFERENCES

- Juan, D. Application of well testing model in fractured-vuggy reservoir in Shunbei Oilfield. *Pet. Geol. Oilfield Dev. Daqing* **2009**, *1–9*, No. 20220.
- Ming, L.; Ping, G.; Wenlin, L. Ordovician carbonate fractured reservoir prediction of Lunnan area in Tarim Basin. *Mar. Origin Pet. Geol.* **2000**, *84–88*.
- Murtaza, M.; Tariq, Z.; Xiaomin, Z.; Al Sheri, D.; Mahmoud, M.; Shahzad Kamal, M. In *Application of a Novel Ecofriendly Okra Powder as Fluid Loss Controller in Water Based Drilling Fluids*, SPE Middle East Oil & Gas Show and Conference, OnePetro, 2021.
- Murtaza, M.; Tariq, Z.; Shahzad Kamal, M.; Mahmoud, M.; Al Sheri, D. In *Application of Okra Mucilage for the Prevention of Shale Swelling*, Abu Dhabi International Petroleum Exhibition & Conference, OnePetro, 2021.
- Tariq, Z.; Shahzad Kamal, M.; Mahmoud, M.; Murtaza, M.; Abdurraheem, A.; Xiaomin, Z. Dicationic surfactants as an additive in fracturing fluids to mitigate clay swelling: A petroph rock mechanical assessment. *ACS Omega* **2021**, *15867–15877*.
- Tariq, Z.; Shahzad Kamal, M.; Mahmoud, M.; Shakil Hussain, S. M.; Hussain, S. R. Novel gemini surfactant as a clay stabilizing additive in fracturing fluids for unconventional tight sandstones: Mechanism and performance. *J. Pet. Sci. Eng.* **2020**, *195*, No. 107917.
- Tariq, Z.; Shahzad Kamal, M.; Mahmoud, M.; Hussain, S. M.; Abdurraheem, A.; Xiaomin, Z. Polyoxyethylene quaternary ammonium gemini surfactants as a completion fluid additive to mitigate formation damage. *SPE Drill. Complet.* **2020**, *35*, 696–706.
- Tariq, Z.; Saleh Aljawad, M.; Hassan, A.; Mahmoud, M.; Al Ramadhan, A. Chelating agents as acid-fracturing fluids: experimental and modeling studies. *Energy Fuels* **2021**, *35*, 2602–2618.
- Tariq, Z.; Hassan, A.; Al Abdralnabi, R.; Saleh Aljawad, M.; Mahmoud, M. Comparative study of fracture conductivity in various carbonate rocks treated with GLDA chelating agent and HCL acid. *Energy Fuels* **2021**, *35*, 19641–19654.
- Tariq, Z.; Bicheng, Y.; Shuyu, S.; Gudala, M.; Saleh Aljawad, M.; Murtaza, M.; Mahmoud, M. Machine learning-based accelerated approaches to infer breakdown pressure of several unconventional rock types. *ACS Omega* **2022**, *7*, 41314–41330.
- Hui, L.; Xuefang, Y.; Lizhi, Z.; Hai, J.; Ju, L.; Zebo, L. Factors of affecting the acid fracturing effect in fracture-cavity carbonate reservoir. *Drill. Prod. Technol.* **2013**, *36*, 53–55.
- Yan, R.; Xiaoming, L.; Xinfei, Y.; Chun, W. Fracability prediction for tight carbonate reservoirs in Chuazhong Moxi area. *Pet. Geol. Oilfield Dev. Daqing* **2018**, *37*, 164–170.
- Xinyong, L.; Yudi, G.; Zhiyuan, L.; Wenzhi, W.; Zhou, Z. An Experimental Study on Evaluation Methods for Fracturing Effect of Fractured-Vuggy Carbonate Reservoir. *Pet. Drill. Tech.* **2020**, *48*, 88–93.
- Bing, H.; Wan, C.; Mian, C.; Peng, T.; Lifeng, Y. Experiments on the non-planar extension of hydraulic fractures in fractured shale gas reservoirs. *Nat. Gas Ind.* **2014**, *34*, 81–86.
- Fisher, M. K.; Wright, C. A.; Davidson, B. M.; Steinsberger, N. P.; Buckler, W. S.; Goodwin, A.; Fielder, E. O. Integrating fracture mapping technologies to improve stimulations in the Barnett shale. *SPE Prod. Facil.* **2005**, *20*, 85–93.
- Maxwell, S. C.; Urbancic, T. I.; Steinsberger, N.; Zinno, R. In *Microseismic Imaging of Hydraulic Fracture Complexity in the Barnett Shale*, SPE Annual Technical Conference and Exhibition, OnePetro, 2002.
- Mayerhofer, M. J.; Lolon, E. P.; Warpinski, N. R.; Cipolla, C. L.; Walser, D.; Rightmire, C. M. What is stimulated reservoir volume? *SPE Prod. Oper.* **2010**, *25*, 89–98.
- Mayerhofer, M. J.; Lolon, E. P.; Youngblood, J. E.; Heinze, J. R. In *Integration of Microseismic-Fracture-Mapping Results with Numerical Fracture Network Production Modeling in the Barnett Shale*, SPE Annual Technical Conference and Exhibition, OnePetro, 2006.
- Zehua, L.; Peng, D.; Chunhe, Y.; Yintong, G.; Longfei, G. Experimental study on mechanical properties and fracability evaluation of carbonate reservoirs. *J. Guangxi Univ.* **2019**, *44*, 1450–1460.
- Fang, S.; Han, W.; Rencai, J. Propagating mechanisms of hydraulic fractures in fracture-cavity carbonate reservoirs. *Pet. Geol. Oilfield Dev. Daqing* **2022**, *41*, 98–106.
- Longfei, H. *Fracture-Cavity Carbonate Directional Fracturing Simulation Test Research*; Chongqing University, 2020. DOI: 10.27670/d.cnki.gcqdu.2020.002029.
- Wenzhi, W. *Study on Cracking Mechanism of Fracture-Cavity Carbonate Hydraulic Fracture in Karst Caves*; China University of Petroleum, 2020.
- Yujie, W.; Zhennan, Z.; Jianye, M.; Bin, Z.; Zhiyuan, L. Impact of cavity on hydraulic fracture in fracture-cavity carbonate reservoir. *Chin. J. Underground Space Eng.* **2019**, *15*, 175–181.
- Jarvie, D. In *Finding Bypassed or Overlooked Pay Zones Using Geo-chemistry Techniques*, International Petroleum Technology Conference, OnePetro, 2008; pp 12–18.
- Rickman, R.; Mullen, M.; Petre, E.; Grieser, B.; Kundert, D. In *A Practical Use of Shale Petrophysics for Stimulation Design Optimization: All Shale Plays Are Not Clones of the Barnett Shale*, SPE Annual Technical Conference and Exhibition, OnePetro, 2008; pp 115–258.
- Yan, J.; Mian, C.; Huaiying, W.; Yang, Y. Study on prediction method of fracture toughness of rock mode II by logging date. *Chin. J. Rock Mech. Eng.* **2008**, *27*, 3630–3635.
- Shurong, L.; Liufang, Z.; Guoxiong, L.; Weiguo, Y. Log evaluation technique of marine carbonate reservoir in northeast Sichuan. *Well Logging Technol.* **2008**, *32*, 337–341.
- Xiaoling, X.; Xinju, J.; Xiang, Z.; Honglei, L.; Yiwei, J. Fracture identification based on multi-information fusion by conventional logging and electrical imaging logging. *Oil Geophys. Prospect.* **2015**, *50*, 542–547.
- Xining, L. *Study on Integrated Logging Evaluation of the Fractured-Vuggy Reservoir*; China University of Petroleum, 2019.
- Shuaishuai, N.; Xiuping, Z.; Jian, S.; Guigang, T.; Chen, C. Experimental study on hydraulic fracturing in clayey-silty hydrate-bearing sediments and fracability evaluation based on multilayer perceptron-analytic hierarchy process. *J. Nat. Gas Sci. Eng.* **2022**, *106*, No. 104735.
- Lili, S.; Yang, J.; Yongming, Y.; Yong, Y.; Aishan, L. A quantification method for shale fracability based on analytic hierarchy process. *Energy* **2016**, *115*, 637–645.
- Zhi, G.; Mian, C.; Yan, J.; Xin, F.; Ning, J. Integrated fracability assessment methodology for unconventional naturally fractured reservoirs: Bridging the gap between geophysics and production. *J. Pet. Sci. Eng.* **2016**, *145*, 640–647.
- Zhengqing, L. A new method for adjusting inconsistency judgment matrix in AHP. *Syst. Eng. Theory Pract.* **2004**, *84–92*.
- Hongwei, Y.; Jun, L.; Gonghui, L.; Yumei, L.; Yan, X.; Geng, T. Quantitative evaluation of shale fracability based on logging data. *Fault-Block Oil Gas Field* **2017**, *24*, 382–386.